

*DEVIATIONS OF THE CROSS SECTIONS FOR SLOW NEUTRON REACTIONS ON
LIGHT NUCLEI FROM THE $1/v$ LAW*

A. A. BERGMAN and F. L. SHAPIRO

P. N. Lebedev Physics Institute, Academy of Sciences, U.S.S.R.

Submitted to JETP editor December 8, 1960

J. Exptl. Theoret. Phys. (U.S.S.R.) **40**, 1270-1281 (May, 1961)

The energy dependence of the cross section ratio for the reactions $\text{Li}^6(n, \alpha)$, $\text{B}^{10}(n, \alpha)$, and $\text{He}^3(n, p)$ are measured at neutron energies $E < 30$ kev. The correction found for the $1/v$ law, expressed as a constant term of the reaction cross section, is -0.03 ± 0.01 b, -0.40 ± 0.03 b, and -1.1 ± 0.2 b for Li^6 , B^{10} , and He^3 , respectively. Available data on the $\text{Li}^7(p, n)$ reaction indicate that the correction of the Be^7 cross section is -61 ± 7 b. The results, which are in good agreement with theoretical predictions, show that thermal neutrons are captured by He^3 into a state with 0^+ spin and parity, and also confirm the hypothesis that thermal-neutron capture by B^{10} and Be^7 proceeds through $1/2^+$ and 2^- states, respectively.

INTRODUCTION

THE detailed investigation of (n, α) and (n, p) reactions on light nuclei is important for the theory of nuclear reactions, the determination of the level schemes of light nuclei, and the technique of measuring neutron flux.

According to the general theory, the cross sections for reactions with neutrons having low energy E can be represented by

$$\sigma_r = \text{const} \cdot E^{-1/2} + \Delta\sigma + \beta' E^{1/2} + \dots$$

The first term of this expansion is the familiar $1/v$ law, while the following terms represent departures from this law.

It can be shown¹ that the negative constant term $\Delta\sigma$ is determined only by the cross section for thermal neutron absorption and by the spin of the reaction channel (nuclear state). The term can therefore be determined without making assumptions regarding parameters and resonance interference. Close resonances produce departures from the $1/v$ law that are proportional in first approximation to the ratio E/E_r (E_r is the resonance energy), as a result of which the cross section contains a term proportional to $E^{1/2}$.

At sufficiently low neutron energies the constant term is the principal correction to the $1/v$ law. This term can be measured if it is sufficiently large (when the cross section for thermal neutron absorption is large) and β' is sufficiently small (in the case of light nuclei, i.e., for low level densities). These conditions are fulfilled in the (n, p) reaction on He^3 and Be^7 , and in the (n, α) reac-

tion on Li^6 and B^{10} . Measurement of $\Delta\sigma$ can be regarded as a method of determining the spin of the channel for these reactions.

In earlier work^{2,3} we measured the energy dependence of the cross section ratios for $\text{Li}^6(n, \alpha)$, $\text{He}^3(n, p)$, and $\text{B}^{10}(n, \alpha)$, at neutron energies $E < 30$ kev. In the present work the ratio for $\text{Li}^6(n, \alpha)$ and $\text{B}^{10}(n, \alpha)$ was measured with considerably greater accuracy. The ratio for $\text{Li}^6(n, \alpha)$ and $\text{He}^3(n, p)$ was also somewhat improved.

We used the data on cross section ratios to determine the constant terms in the cross sections. The available data on $\text{Be}^7(n, p)$ and $\text{Li}^7(p, n)$ will be used in the same way.

The data also lead to certain conclusions concerning the energy dependence of the individual reactions and the resonances responsible for the thermal cross sections of these reactions. These questions have been discussed in our earlier papers^{2,3} and will be touched on here only in connection with new data in the literature.

The cross section ratios were measured by means of a neutron spectrometer based on slowing-down times in lead. Since the technique was not explained in references 2 and 3, it will be described here.

EXPERIMENTAL TECHNIQUE

Measurements are obtained with a slowing-down-time-in-lead neutron spectrometer as follows.* A burst of fast neutrons lasting $0.5 \mu\text{sec}$ is generated

*For more details see reference 4.

within a large lead cube weighing ~ 110 tons at the beginning of each 1600- μ sec cycle. At the time t after the burst neutrons are slowed down to the average energy

$$\bar{E} = 186/(t + 0.5)^2 \text{ kev}, \quad (1)$$

where t is the slowing-down time in microseconds.

For large slowing-down times ($t \geq 14 \mu\text{sec}$) the energy spectrum of the slowed neutrons is very nearly Gaussian with $\sim 14\%$ rms spread around the mean.^{2,4} For shorter slowing-down times the neutron spectrum is broader; thus for $t = 4 \mu\text{sec}$ the rms spread is $\sim 30\%$ and for $t = 2.5 \mu\text{sec}$ it is $\sim 35\%$.¹⁴

As a result of leakage from the lead cube and capture in lead, neutron density decreases with slowing-down time as

$$\rho(t) = \text{const} \cdot (t + 0.5)^{-\alpha} e^{-t/T}, \quad (2)$$

with $\alpha = 0.35$ and $T = 890 \mu\text{sec}$ for the given lead cube.

Several measuring channels in the lead cube at different distances from the target contain detectors registering reactions induced by slowed-down neutrons. For a sufficiently thin-walled detector (with respect to neutron absorption) the counting rate is

$$J(t) = \text{const} \cdot \int n(E, t) v \sigma(E) \eta(E) dE \\ = \text{const} \cdot \rho(t) v(\bar{E}) \sigma(\bar{E}) \eta(\bar{E}) K(\bar{E}), \quad (3)$$

where $n(E, t) dE$ is the neutron density from E to $E + dE$ at slowing-down time t , v is the neutron velocity, $\sigma(E)$ is the reaction cross section, η is the registration efficiency of the nuclear reaction in the detector. For neutron energies much smaller than the reaction energy η is practically independent of energy. K is a correcting factor taking into account the fact that the mean value $v\sigma(E)\eta(E)$ is not generally equal to $v(\bar{E})\sigma(\bar{E})\eta(\bar{E})$.

The broader the neutron energy spectrum $n(E, t)$, and the more the cross section departs from the $1/v$ law, the greater the difference between K and unity. Calculations show that $K(E)$ is practically unity for the investigated reactions when $\bar{E} < 30$ kev. Therefore the counting-rate ratio of two detectors at the same point in the cube is proportional, except for a small correction, to the ratio of the reaction cross sections for energy equal to the mean neutron energy $\bar{E}(t)$. By measuring the counting-rate ratio of the two detectors as a function of the slowing-down time, we obtain the energy dependence of the cross section ratio.

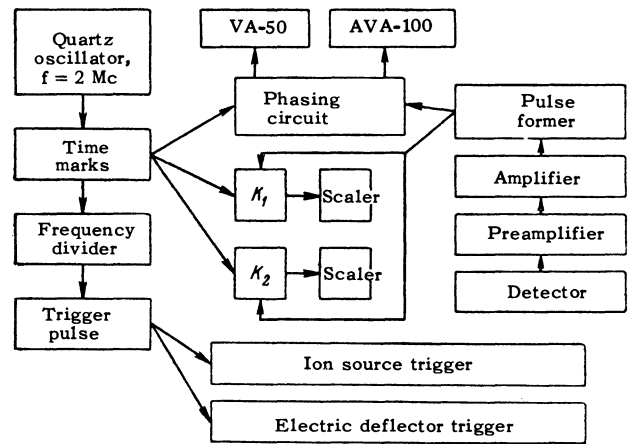


FIG. 1. Block diagram of circuit for slowing-down-time-in-lead neutron spectrometer. VA-50 and AVA-100 are 50-channel and 100-channel time analyzer; K_1 and K_2 are single-channel time analyzers.

APPARATUS

The neutron spectrometer (Fig. 1) was controlled by a quartz oscillator with frequency $f = 2$ Mc, the sinusoidal oscillations of which were transformed into synchronizing time marks and trigger pulses. Trigger pulses went to the time analyzers (see below), and through the delay lines also actuated the pulse circuits of the ion source and of the electric cutoff (deflector) for the ion beam.

Detector pulses were fed to the remote preamplifier and to the broad-band amplifier, discriminator, and time analyzers. The upper transmission limit of the entire amplifying circuit was 5 Mc.

In the present work we used a 50-channel time analyzer VA-50 with 0.5- μ sec channels, two single-channel time analyzers, and a 100-channel time analyzer AVA-100 with channel widths varying from 1 to 80 μ sec.

The 50-channel analyzer was equipped with a phasing circuit which phased shaped pulses in accordance with the synchronizing time markings, shifting them to the middle of each channel. This resulted in rigidly identical analyzer channel widths with no gaps between channels. The 100-channel analyzer was similarly equipped. The dead time determined by the pulse-phasing circuit was 2.5 μ sec. In addition, counting losses of the analyzer channels were determined from the dead time of the electromechanical registers ($\tau_{\text{mech}} = 0.01$ sec) that recorded pulses from the individual channels.

The single-channel time analyzers, each of which fed two parallel scalars with 0.5- μ sec re-

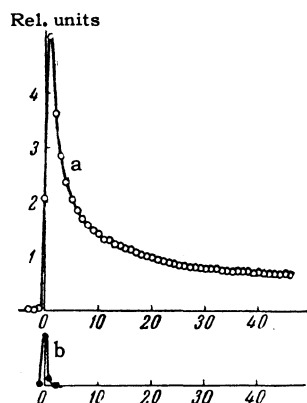


FIG. 2. a—counting rate (in relative units) of boron counter in channel of lead block vs slowing-down time; b—the same dependence for a high threshold of pulse-height discrimination. This curve represents the shape of the fast-neutron burst. Serial numbers of the analyzer channels (each $0.5 \mu\text{sec}$ wide) are plotted on the horizontal axis.

solving time, were adjusted and synchronized with respect to the pulse registration interval and the time from the start of the cycle to that interval.

The operating cycle of the spectrometer was $1600 \mu\text{sec}$ (625 bursts per sec). This provided for sufficiently small density of slowed neutrons remaining after each cycle.

The first two channels of the VA-50 analyzer registered only reactions induced by neutrons of the preceding cycle. The time stability of the spectrometer components was thus monitored from the position of the neutron burst (Fig. 2). The VA-50 analyzer covered neutron energies above 400 eV, while the AVA-100 analyzer covered lower energies.

The measuring interval of the two single-channel time analyzers K_1 and K_2 was $200 \mu\text{sec}$, located 100 and $1400 \mu\text{sec}$, respectively, from the start of the cycle. The high counting rate of K_1 represented ~ 8 -eV neutrons, with very little departure from $1/v$. Therefore the cross section ratio given by K_1 provides a good reference point for measurements.

Analyzer K_2 was operated at the end of the cycle, where the intensity was about one-ninth of that for K_1 . This permitted convenient monitoring of the background, since even a small background increases appreciably the ratio of K_2 to K_1 counts.

The correct functioning of each analyzer and its dead time were checked regularly both electronically and by means of constant sources.

DETECTORS

In the present work the ratio between the cross sections for $\text{Li}^6(n, \alpha)$ and $\text{B}^{10}(n, \alpha)$ was meas-

ured by two identical proportional counters (Fig. 3) with 25-mm cathode diameter and 1.3-mm wire diameter,* which were filled with argon at 230 mm, CO_2 at 12 mm, and air at 7 mm Hg. One counter contained a 0.22-mg/cm^2 layer of natural boron, while the other contained a 1.13-mg/cm^2 layer of Li^6F . These homogeneous thin layers were vacuum deposited on aluminum foils. The principal requirement was short pulse delay.

For the purpose of measuring retardation the detectors were inserted into a channel of the lead cube close to the target, where there was a large flux of 14-MeV primary neutrons. Pulses from slow neutrons (i.e., after long slowing-down times) were cut off by raising the height-discrimination threshold. The time analyzer then traced the shape of the neutron burst (Fig. 2).

The burst registered by the detectors was compared with that registered by a fission ionization chamber containing layers of natural uranium.† The electrode gap in this chamber was 3 mm, and its gas filling was 95% argon and 5% CO_2 , with operation at $\mathcal{E}/p \sim 7 \text{ v/cm-mm Hg}$. The large pulses from the fission chamber permitted us to use the initial leading-edge segment for registration. We can therefore assume that the registration lag of the center of gravity of the neutron burst in the fission chamber does not exceed $0.03 \mu\text{sec}$. In all instances the detectors were less than $0.07 \mu\text{sec}$ behind the fission chamber.

Measurements with different cutoff thresholds indicated that there were practically no additional time shifts of electronic origin between the compared detectors.

MEASUREMENTS

If the cross section ratios are to be measured with accuracy better than 1%, in addition to obtaining sufficient data it is necessary to take all steps that will reduce both random and systematic errors. Measurements were performed in the following order.

- 1) Gas multiplication in the compared counters was such as to produce equal mean pulses. The detectors were connected alternately to a single electronic channel.

*This diameter permitted a higher counter operating voltage for the purpose of producing higher electron mobility. The gas amplification factor was about 10.

†The fission of U^{238} is induced only by 1-MeV neutrons, i.e., by primary neutrons and those undergoing inelastic scattering on lead nuclei, which does not introduce any perceptible retardation. A small admixture of U^{235} was insignificant for the present measurements.

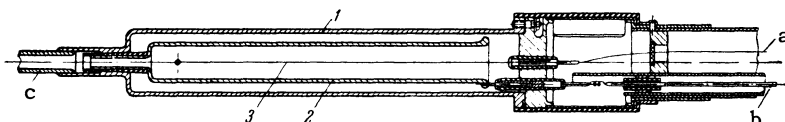


FIG. 3. Diagram of counters used to register $B^{10}(n, \alpha)$ and $Li^6(n, \alpha)$ reactions. 1—thin steel shell; 2—cathode (with interior lining of aluminum foil bearing deposited layer); 3—1.3-mm counter wire; a—lead to preamplifier; b—high-voltage lead; c—tube to stopcock.

2) The counting rates were such that counting losses did not exceed 1.5% and were as close to equality as possible in the two counters.

3) The two counters were used alternately for periods of 40 to 60 min during a total measuring time of a few days. The detectors were placed in exactly the same position in the lead block.

4) The fission chamber measured systematically the position of the neutron burst in the multi-channel analyzers.

5) Backgrounds were measured systematically by omitting the electric cutoff pulse, i.e., when the ion beam did not impinge on the zirconium-tritium target.

RESULTS

Figure 2 shows the counting rate of the boron detector as a function of slowing-down time, as obtained in one of the 10 runs. The slowing-down time was measured from the center of gravity of the neutron burst, as determined by the fission chamber and corrected for lag of the boron detector after the fission chamber. We also used measurements in the course of which the neutron bursts did not drift in the VA-50 analyzer and the background was very small and stable. Less than 20% of the measurements were rejected.

For each run, after introducing corrections for the background and counting loss, the counting-rate ratio of the two detectors was determined (Fig. 4). For each time channel the mean ratio for the different runs was calculated, with normalization to the ratio obtained with K_1 . The rms spread

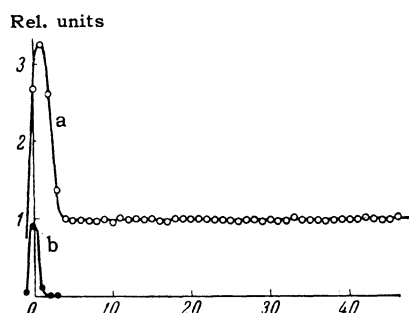


FIG. 4. a—counting-rate ratio of boron and lithium counters vs slowing-down time; b—shape of fast-neutron burst measured by uranium fission chamber. Serial numbers of the 0.5- μ sec analyzer channels are plotted on the horizontal axis.

of the normalized ratios around the mean value was close to the statistical spread.

The mean ratio of the counts from analyzers K_2 and K_1 , corrected for the background, was smaller by $1.85 \pm 0.35\%$ for the Li^6F layer than for the boron counter. This difference was incomparably larger than could be expected from departures from the $1/v$ law. The cause of the discrepancy lay in different degrees of neutron absorption by the layers and by the incompletely identical counters. The observed absorption effect was several times greater than absorption in a single transit. This was confirmed by special measurements with interchangeable absorbers, which showed that the observed absorption was proportional to the neutron slowing-down time. Therefore the correction for absorption during short slowing-down times (in channels of the VA-50 analyzer) was negligibly small.

After introducing the corrections listed in the table, including those for absorption, and using Eq. (1) to convert from slowing-down time to energy, the curves in Figs. 5 and 6 were obtained, showing the energy dependence of the cross section ratio for $Li^6(n, \alpha)$ and $B^{10}(n, \alpha)$ and for $Li^6(n, \alpha)$ and $He^3(n, p)$.

The solid curves in Figs. 5 and 6 are parabolas plotted by least squares. The parameters of these parabolas are discussed below; the errors shown include the rms random errors and an estimate of possible systematic errors.

The experimental results represented in Figs. 5 and 6 do not include a correction for the depend-

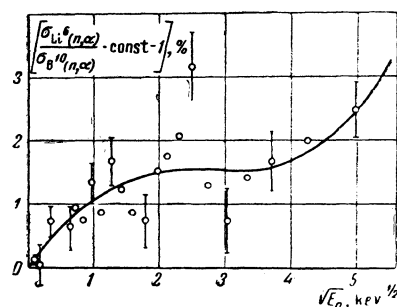


FIG. 5. Departure of cross section ratio for $Li^6(n, \alpha)$ and $B^{10}(n, \alpha)$ from its value in the thermal region vs square root of neutron energy. The solid curve represents Eq. (7), plotted through the experimental points by least squares.

Corrections of the cross section ratios for $\text{Li}^6(n, \alpha)$ and $\text{B}^{10}(n, \alpha)$, and for $\text{Li}^6(n, \alpha)$ and $\text{He}^3(n, p)^*$

$\sqrt{E_n}, \text{keV}^{1/2}$	$\sigma_{\text{Li}^6}/\sigma_{\text{B}^{10}}$		$\sigma_{\text{Li}^6}/\sigma_{\text{He}^3}$			
	4.98	3.33	0.09 (analyzer K ₁)	5.26	2.73	0.09 (analyzer K ₁)
Correction for neutrons from D-D reaction**, %	-0.15±0.10	0	0	-1.25±0.2	-0.35±0.05	0
Correction for counting loss, %	0.98±0.25	-0.09±0.02	0	0.55±0.1	0	0
Correction for background (except D-D neutron background), %	0	0	0.08	0	0	0.06
Correction for absorption, %	0	0	0.23±0.04	0	0	none
Correction for neutron dispersion, %	-0.46	0	0	-0.13	0	0
Correction for instrumental time resolution, %	-0.26	0	0	-0.4±0.2	0	0
Total	0.11±0.35	-0.09±0.02	0.31±0.04	-1.2±0.4	-0.35±0.05	0.06

*The correction for neutrons of the preceding cycle was negligibly small.

**Neutrons from the D-D reaction appeared when the ion beam was deflected by the electric cutoff and struck the wall of the target tube.

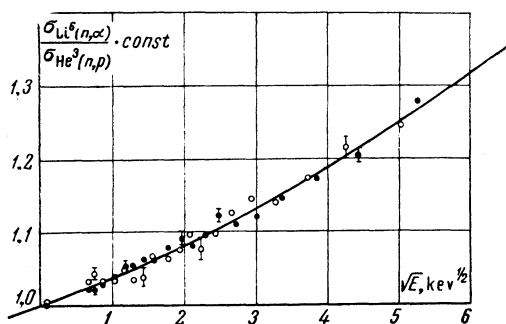


FIG. 6. Cross section ratio for $\text{Li}^6(n, \alpha)$ and $\text{He}^3(n, p)$ vs square root of neutron energy. The curve is normalized to unity for $E_n = 0$. \circ - first (preliminary) run; \bullet - second run; solid curve - parabola (12) plotted by least squares from the second run.

ence of registration efficiency on neutron energy. This correction is proportional to neutron energy, affecting only one (β) of the parabola parameters and was therefore introduced directly into the values of this parameter (see footnote on page 897 and the footnote under this column).

DISCUSSION OF RESULTS

1. As has been shown in reference 1, the cross section for a reaction induced by S neutrons (with orbital moment $l = 0$) can be represented by*

$$\sigma_r = \frac{(\sigma_r E^{1/2})_0 E^{-1/2}}{1 + \alpha E^{1/2} + \beta E + \gamma E^2 + \dots} = (\sigma_r E^{1/2})_0 (E^{-1/2} - \alpha + \beta^* E^{1/2} + \dots), \quad (4)$$

Neutron capture with $l \geq 1$ contributes to higher terms of the expansion, beginning with $\beta^ E^{1/2}$.

where

$$\alpha = \frac{m}{\pi \hbar^2} \left(\frac{A}{A+1} \right)^2 (\sigma_r E^{1/2})_0 [x_-^2 / g_- + (1 - x_-)^2 / (1 - g_-)], \quad (5)$$

m is the neutron mass, A is the mass number of the target nucleus, $(\sigma_r E^{1/2})_0$ is the value of $\sigma_r E^{1/2}$ for $E \rightarrow 0$ (i.e., practically for thermal neutrons), $g_- = I / (2I + 1)$ is the statistical weight of the reaction channel with spin $J = I - 1/2$ (I is the target-nucleus spin), and x_- is the relative contribution of this state to the cross section for thermal neutrons.

Equation (4) is applicable to low neutron energies, when the terms beginning with γE^2 are small compared with 1 and βE . The constant term in the cross section, which was discussed above, is related to α by

$$\Delta \sigma = -\alpha (\sigma_r E^{1/2})_0. \quad (6)$$

The measured cross section ratio for Li^6 and B^{10} (Fig. 5) is well represented by

$$\sigma_{\text{Li}} / \sigma_{\text{B}} = \text{const} [1 + (\alpha_{\text{B}} - \alpha_{\text{Li}}) E^{1/2} + \beta_{\text{Li/B}} E + \gamma_{\text{Li/B}} E^2] \quad (7)$$

with the following constant coefficients:

$$\begin{aligned} \alpha_{\text{B}} - \alpha_{\text{Li}} &= (1.43 \pm 0.20) \cdot 10^{-2} \text{ keV} \\ \beta_{\text{Li/B}} &= -(0.37 \pm 0.09) \cdot 10^{-2} \text{ keV}^* \\ \gamma_{\text{Li/B}} &= (0.73 \pm 0.27) \cdot 10^{-4} \text{ keV} \end{aligned}$$

Equation (7) follows directly from (4) when we neglect all terms of higher order than E^2 as well as

*After corrections for the variation of registration efficiency with neutron energy, we have $\beta_{\text{Li/B}} = -(0.35 \pm 0.09)$.

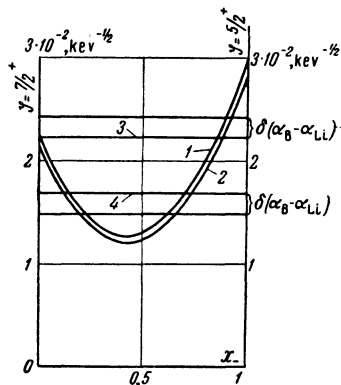


FIG. 7. Dependence of the coefficient α_B on the ratio of contributions by states with spin and parity $5/2^+$ and $7/2^+$. The two curves correspond to two values of the thermal cross section for $B^{10}(n, \alpha)$: $1-\sigma = 4000$ b; $2-\sigma = 3800$ b. The straight lines represent experimental values of α_B for the two limits of α_{Li} : $3 - \alpha_{Li} = 0.80 \times 10^{-2} \text{ keV}^{-1/2}$; $4 - \alpha_{Li} = 0.26 \times 10^{-2} \text{ keV}^{-1/2}$. $\delta(\alpha_B - \alpha_{Li})$ is the experimental error of α .

the $E^{3/2}$ term, which must be very small since it is absent rigorously from the denominator in (4) and because σ_{Li}/σ_B is close to a constant.

Using the cross sections for thermal neutron absorption,^{5,6} we find that for Li^6 ($I = 1^+$), depending on our hypothesis regarding the ratio of the contributions from the states with spins $1/2$ and $3/2$ to the thermal cross section, the variation of α is given by

$$0.26 \cdot 10^{-2} \leq \alpha_{Li} \leq 0.80 \cdot 10^{-2} \text{ keV}^{-1/2}. \quad (8)$$

Combining this result with the measured value of $\alpha_B - \alpha_{Li}$, we obtain

$$1.69 \pm 0.20 \leq \alpha_B \cdot 10^2 \leq 2.23 \pm 0.20. \quad (9)$$

In Fig. 7 these limits are compared with the values of α_B calculated for different ratios of the contributions from the channels with spins $5/2$ and $7/2$. The spin and parity of the B^{10} ground state is 3^+ .*

The experimental results appear to be in agreement with each of the two hypotheses:

a) Neutrons are captured principally into the state $J = 5/2^+$ with an appreciable number going to the state $J = 7/2^+$, or

b) Neutrons are captured into the state $J = 7/2^+$ with none or very few going into the state $J = 5/2^+$.

Recent measurements of the γ -ray spectrum resulting from thermal-neutron capture in B^{10} ,⁸ show that capture proceeds predominantly through the spin $7/2$ channel. The second of the two given possibilities is thus realized.

*The literature gives two values of the thermal cross section for $B^{10}(n, \alpha)$: ~ 3800 b^{5,7} and ~ 4000 b.⁶ We assume $\sigma = 3900 \pm 100$ b.

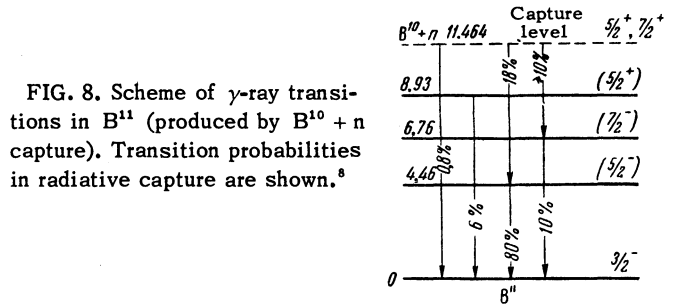


FIG. 8. Scheme of γ -ray transitions in B^{11} (produced by $B^{10} + n$ capture). Transition probabilities in radiative capture are shown.⁸

2. The measurements given in reference 8 (represented in Fig. 8) make it possible to estimate the contribution x_- of the $5/2^+$ state to the capture of thermal neutrons by B^{10} , which in turn permits the calculation of α_B , so that α_{Li} can be determined from the experimental values of $\alpha_B - \alpha_{Li}$.

Capture into the state $J = 5/2^+$ should lead to E1 transitions to the B^{11} ground state with the emission of 11.43-Mev quanta. The number of these transitions from the $5/2^+$ state per capture is, in any event, smaller than the total yield of 11.43-Mev quanta, i.e.,

$$x_- \Gamma_\gamma / \Gamma < 8 \cdot 10^{-3} \sigma_\gamma / \sigma,$$

where σ is the total absorption cross section, σ_γ is the cross section for radiative capture, and Γ_γ and Γ are the partial and total widths of the compound nucleus in the state $J = 5/2^+$.

Similarly, for the transition from the $7/2^+$ capture state to the 4.46-Mev level of B^{11} ($E_{\gamma'} = 6.98$ Mev) we have

$$(1 - x_-) \Gamma_{\gamma'} / \Gamma' \approx \Gamma_{\gamma'} / \Gamma' = 0.18 \sigma_{\gamma'} / \sigma.$$

Assuming that this is an electric dipole transition, we take $\Gamma_{\gamma'} / \Gamma_\gamma = (E_{\gamma'} / E_\gamma)^3$. Assuming, furthermore, $\Gamma = \Gamma'$, we obtain $x_- < 1\%$.*

Substituting in (5), with a certain amount of margin, $x_- = 3 \pm 3\%$, we obtain

$$\alpha_B = (2.06 \pm 0.14) \cdot 10^{-2} \text{ keV}^{-1/2}. \quad (10)$$

Using the measured value of $\alpha_B - \alpha_{Li}$, we thus arrive at

$$\alpha_{Li} = (0.63 \pm 0.24) \cdot 10^{-2} \text{ keV}^{-1/2}. \quad (11)$$

Figure 9 shows that the value of α_{Li} agrees better with the hypothesis that thermal-neutron capture by Li^6 proceeds predominantly through the state $J = I - 1/2 = 1/2$. However, the calculation is insufficiently accurate to furnish a decisive result.

*If $E_\gamma = 6.98$ Mev does not represent an E1 transition, the estimated value of x_- will be still smaller.

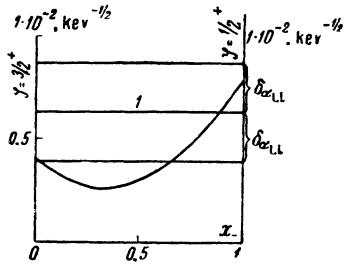


FIG. 9. Dependence of the coefficient α_{Li} on the ratio of contributions from the states with spin and parity $3/2^+$ and $1/2^+$. The straight line 1 is the experimental value of α_{Li} . $\delta(\alpha_{Li})$ is the experimental error in α_{Li} .

According to (6), (10), and (11) the constant terms in the cross sections for boron and lithium are

$$\Delta\sigma_{B^{10}} = -0.40 \pm 0.03 \text{ b}, \quad \Delta\sigma_{Li} = -0.03 \pm 0.01 \text{ b}.$$

The $B^{10}(n, \alpha)$ reaction is known to have two branches, with Li^7 formed in its ground and excited states, respectively. For thermal neutrons the yield ratio of the two branches is 6.2%.⁹ The value of α_B given above pertains to the energy dependence of the total cross section. By measuring the energy dependence of the branching ratio we could determine α for the branch in which ground-state Li^7 is produced and determine the relative contributions of the $5/2^+$ and $1/2^+$ channels for this branch.

3. The coefficients β and γ in (4), which gives the energy dependence of the reaction cross section, are principally determined by the compound-nucleus states excited by S neutrons.^{1,2*} The coefficients are large if the levels responsible for the thermal cross section are close to the neutron binding energy; otherwise they are small. $\beta > 0$ and $\beta < 0$ for levels lying below and above the binding energy, respectively. Li^7 has no levels close to the binding energy,[†] so that β_{Li} and γ_{Li} must be small. Since in (7) $\beta_{Li/B} \approx \beta_B - \beta_{Li}$ and $\gamma_{Li/B} \approx \gamma_B - \gamma_{Li}$, our measured values of $\beta_{Li/B}$ and $\gamma_{Li/B}$ are close to β_B and γ_B , respectively. The sign and magnitude of β and the magnitude of γ indicate that the thermal cross section of B^{10} is determined mainly by the level or levels located hundreds of kev above the neutron binding energy in B^{11} . This agrees with the hypothesis that the 11.46-Mev and 11.68-Mev levels of B^{11} are responsible for the thermal cross section.¹¹

4. In earlier work³ we measured the energy dependence of the cross section ratio for $Li^6(n, \alpha)$ and $He^3(n, p)$, which is well represented by

$$\sigma_{Li}/\sigma_{He} = \text{const} \cdot [1 + (\alpha_{He} - \alpha_{Li}) E^{1/2} + \beta_{Li/He} E] \quad (12)$$

with the constants

*Including the near-threshold state discussed by Baz'.¹⁰

†The nearest level excited by S neutrons is 830 kev below the neutron binding energy in Li^7 .⁹

$$\alpha_{He} - \alpha_{Li} = (3.54 \pm 0.5) 10^{-2} \text{ kev}^{-1/2},$$

$$\beta_{Li/He} = (2.87 \pm 1.3) 10^{-3} \text{ kev}^{-1}.*$$

Making use of (11), we now obtain

$$\alpha_{He} = (4.17 \pm 0.55) \cdot 10^{-2} \text{ kev}^{-1/2},$$

$$\Delta\sigma_{He} = -1.1 \pm 0.2 \text{ b}.$$

α_{He} is close to the largest possible value, $(4.65 \pm 0.25) \times 10^{-2} \text{ kev}^{-1/2}$, which is obtained if the He^3 cross section in the thermal region⁵ is determined completely by the 0^+ reaction channel. This differs markedly from the value $(1.65 \pm 0.09) \times 10^{-2} \text{ kev}^{-1/2}$ corresponding to the 1^+ channel, which makes the contribution $x_- = 6 \pm 6\%$.

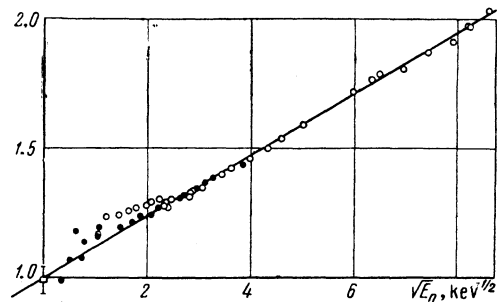


FIG. 10. The plot of $(\sigma E^{1/2})^{-1/2} = f(E^{1/2})$ for the $Be^7(n, p)$ reaction. O — from measurements of $Li^7(p, n)$ with a 9.3-mg/cm² LiF target;¹³ ● — the same with a 6.5-mg/cm² target. □ — data in reference 9.

We note that this conclusion, although based on measurements of the cross section ratio for $Li^6(n, \alpha)$ and $He^3(n, p)$, is not actually associated with any hypotheses regarding the energy dependence of the cross section for the first of these reactions. Only the experimental value (11) of α_{Li} is used, or, if convenient, the equivalent theoretical inequality (8).

We must therefore reject the argument of Bame and Cubitt,¹² who obtained a considerable departure from the $1/v$ law in measurements of the $Li^6(n, \alpha)$ cross section, which, combined with the value of σ_{Li}/σ_{He} in reference 3 indicates that the $1/v$ law is valid for He^3 . The large value of α_{He} inevitably leads to a considerable departure from $1/v$ for the $He^3(n, p)$ reaction. At the same time, the low accuracy (10–15%) of Bame and Cubitt's measurements throws doubt on the reliability of their conclusions. In addition, reference 14 contains data indicating that the cross section for $B^{10}(n, \alpha)$ obeys the $1/v$ law within about 5% up to $E \sim 100$ kev. Since, according to the present

*After introducing corrections for the variation of registration efficiency with neutron energy, we obtain

$$\beta_{Li/He} = (3.2 \pm 1.4) \cdot 10^{-3} \text{ kev}^{-1}.$$

work, the cross sections for $\text{Li}^6(n, \alpha)$ and $\text{B}^{10}(n, \alpha)$ vary in an identical manner (within 2%) for $E \leq 25$ keV, it follows that for the first of these reactions the departure from $1/v$ should not exceed 7%. A conclusive determination of the energy dependence of the $\text{Li}^6(n, \alpha)$ cross section requires that the measured cross section ratio be supplemented by a precision measurement of the energy dependence of one of the (n, α) or (n, p) reactions. We are preparing to obtain these measurements.

5. The $\text{Be}^7(n, p)$ reaction should exhibit an especially large departure from $1/v$, since Be^7 is characterized by a very large thermal-neutron absorption cross section $\sigma_r = 51\,000 \pm 6\,000$ b.* The energy dependence of the cross section for this reaction can be obtained by measuring the cross section for the reverse reaction¹³ $\text{Li}^7(p, n)$ and using the reciprocity theorem. An analysis of these data in accordance with (4) shows that within error limits α and β satisfy

$$\beta = (\alpha/2)^2. \quad (13)$$

Equation (13) is easily confirmed¹ under the following conditions: a) $\text{Re } f = 0$ or $(\text{Re } f)^2 \ll (\text{Im } f)^2$, where f is the logarithmic derivative of the neutron wave function on the nuclear surface, b) $\text{Im } f = \text{const}$, and c) $x_- = 0$ or $x_- = 1$, or $x_- = g_- = 0.375$. In this case (4) has the very simple form

$$\sigma_r E^{1/2} = (\sigma_r E^{1/2})_0 / \left(1 + \frac{1}{2} \alpha E^{1/2}\right)^2. \quad (14)$$

Figure 10 shows that the experimental results^{13,15} agree well with (14) when

$$\alpha = 0.24 \pm 0.01 \text{ keV}^{-1/2}. \quad (15)$$

This corresponds to two possible values of the relative contribution to the thermal cross section by the state with $J = I = \frac{1}{2} = 1$, which are $x_- = 0 \pm 0.07$ and 0.75 ± 0.07 . We must reject the second value, which would result in a large departure from (14).† Thus thermal neutron capture by Be^7 proceeds practically entirely through the 2^- channel. This conclusion also follows from an analysis based on resonance theory,¹³ according to which the cross section for $\text{Be}^7(n, p)$ at low neutron energies is determined by a very broad 2^- level, close to the neutron binding energy in Be^8 . Baz'¹⁰ regards this level as a special near-threshold state.

*This value was obtained by averaging Hanna's data¹⁵ for the total absorption cross section ($48\,000 \pm 9\,000$ b) and for the (n, p) cross section ($53\,000 \pm 8\,000$ b).

†We reject the unlikely possibility that (13) results from an accidental coincidence of independent parameters, rather than from the fulfillment of conditions a), b), and c).

The constant term in the cross section of Be^7 is $\Delta\sigma_{\text{Be}} = -61 \pm 7$ b. If neutron capture through the state with $J = 1^-$ is entirely absent, it follows from (15) that the thermal cross section of Be^7 is $51\,000 \pm 2100$ b.

The authors thank A. N. Volkov and A. M. Klambukov, who perfected and adjusted the electronic equipment of the spectrometer for slowing-down time measurements.

¹F. L. Shapiro, JETP **34**, 1648 (1958), Soviet Phys. JETP **7**, 1132 (1958).

²Bergman, Isakov, Popov, and Shapiro, JETP **33**, 9 (1957), Soviet Phys. JETP **6**, 6 (1958).

³Bergman, Isakov, Popov, and Shapiro, Ядерные реакции при низких и средних энергиях (Nuclear Reactions at Low and Intermediate Energies) Trans. All-Union Conference, 1957, Acad. Sci. Press, 1958, p. 17; Proc. International Conference on Neutron Interactions, Columbia Univ., N.Y., 1957, p. 191.

⁴Bergman, Isakov, Popov, and Shapiro, *ibid.*, p. 140; Bergman, Isakov, Murin, Shapiro, Shtranikh, and Kazarnovskii, Trans. of the Geneva Conference **4**, 166, 1955.

⁵D. J. Hughes and R. B. Schwartz, Neutron Cross Sections, BNL-325, 2nd ed., 1958.

⁶Hughes, Maqurno, and Brussel, Supplement 1 to BNL-325, 1960.

⁷Safford, Taylor, Rustad, and Havens, Bull. Am. Phys. Soc. **5**, 288 (1960).

⁸G. A. Bartholomew and P. J. Campion, Can. J. Phys. **35**, 1347 (1957); F. Ajzenberg-Selove and T. Lauritsen, Nuclear Phys. **11**, 1 (1959).

⁹G. C. Hanna, Phys. Rev. **80**, 530 (1950).

¹⁰A. I. Baz', Advances in Physics (Supplement of Phil. Mag.) **8**, 349 (1959).

¹¹H. Bichsel and T. W. Bonner, Phys. Rev. **108**, 1025 (1957).

¹²S. J. Bame and R. L. Cubitt, Phys. Rev. **114**, 1580 (1959).

¹³R. L. Macklin and J. H. Gibbons, Phys. Rev. **109**, 105 (1958).

¹⁴Bilpuch, Weston, and Newson, Ann. Phys. **10**, 456 (1960).

¹⁵R. C. Hanna, Phil. Mag. **46**, 381 (1955).